Cardiac troponin T is essential in sarcomere assembly and cardiac contractility

Amy J. Sehnert[1,2], Anja Huq[1], Brant M. Weinstein[3], Charline Walker[4], Mark Fishman[5] & Didier Y.R. Stainier[1]

Published online: 22 April 2002, DOI: 10.1038/ng875

Mutations of the gene (*TNNT2*) encoding the thin-filament contractile protein cardiac troponin T are responsible for 15% of all cases of familial hypertrophic cardiomyopathy, the leading cause of sudden death in young athletes[1,2]. Mutant proteins are thought to act through a dominant-negative mode that impairs function of heart muscle[3]. *TNNT2* mutations can also lead to dilated cardiomyopathy, a leading cause of heart failure[4]. Despite the importance of cardiac troponin T in human disease, its loss-of-function phenotype has not been described. We show that the zebrafish *silent heart* (*sih*) mutation affects the gene *tnnt2*. We characterize two mutated alleles of *sih* that severely reduce *tnnt2* expression: one affects mRNA splicing, and the other affects gene transcription. Tnnt2, together with α-tropomyosin (Tpma) and cardiac troponins C and I (Tnni3), forms a calcium-sensitive regulatory complex within sarcomeres[5]. Unexpectedly, in addition to loss of Tnnt2 expression in *sih* mutant hearts, we observed a significant reduction in Tpma and Tnni3, and consequently, severe sarcomere defects. This interdependence of thin-filament protein expression led us to postulate that some mutations in *tnnt2* may trigger misregulation of thin-filament protein expression, resulting in sarcomere loss and myocyte disarray, the life-threatening hallmarks of *TNNT2* mutations in mice and humans[6,7].

Forward genetics in zebrafish has led to the identification of several mutations affecting cardiac contractility[8,9]. The most severe and heart-specific of these is *sih*, which causes a non-contractile heart phenotype (Fig. 1). Skeletal and smooth-muscle function remain intact in *sih* mutant embryos, as evidenced by their ability to hatch, swim and show gut peristalsis. One γ-ray–induced allele (sih^{b109}) and one chemically induced allele (sih^{tc300b}) exist[8]. Both of these mutated alleles are fully penetrant and recessive lethal, and sih^{b109} and sih^{tc300b} mutant embryos are phenotypically indistinguishable. As *sih* embryos age, pericardial edema develops, the endocardium peels away from the myocardium and the embryos die around seven days post fertilization. Until that time, embryos survive on diffused oxygen and are not dependent on circulating blood[10].

To determine whether the *sih* phenotype is due to defects in cellular excitation or excitation–contraction coupling, we devised a new assay using the fluorescent calcium indicator Ca^{2+} green. In wildtype hearts, a wave of fluorescence representing Ca^{2+} influx into cardiomyocytes precedes the contractile wave and progresses from the venous to the arterial end (see Web Movie A and Web Note A online). In mutant hearts, we also observed regular waves of fluorescence, but these were not followed by contraction (Fig. 2*a–d*). On the basis of this assay, cellular excitation seemed to be intact in mutant cardiomyocytes, indicating that the absence of contractility results from abnormalities downstream of calcium influx.

The alignment of thick and thin filaments into sarcomeres creates a highly ordered ultrastructural pattern that is evident in wildtype zebrafish cardiomyocytes at 48 hours post-fertilization (hpf) by electron microscopy (Fig. 2*e*). By contrast, sih^{b109} mutant cardiomyocytes at this stage show only a few loosely organized thick filaments near the cell periphery and no thin filaments or electron dense Z-disks (Fig. 2*f–h*). These results suggest that *sih* influences the assembly and stability of thin filaments, which are required for sarcomere assembly.

Using whole-mount immunohistochemistry, we examined the expression of thick- and thin-filament contractile proteins in wildtype and *sih* mutant embryos from both alleles (Fig. 3). Consistent with the presence of thick filaments as seen by electron microscopy, myosin heavy chain is expressed at wildtype levels throughout the mutant heart tubes (Fig. 3*b*). α-cardiac

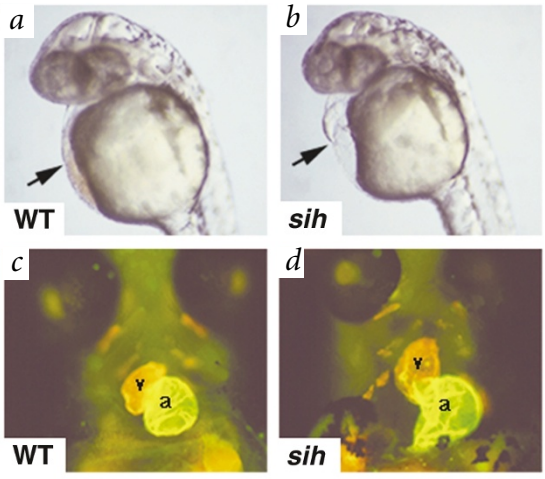

Fig. 1 *sih* phenotype. ***a***,***b***, Wildtype (*a*) and *sih* mutant (*b*) embryos at 32 hpf. A sih^{b109} mutant embryo is shown; sih^{tc300b} mutants appear identical. Note blood cells in the heart of the wildtype embryo (*a*, arrow) and lack of blood cells in the heart and pericardial edema in the sih^{b109} mutant embryo (*b*, arrow). No intermediate heterozygote phenotype was observed. ***c***,***d***, Ventral view; anterior to the top. Normal cardiac looping and chamber differentiation is seen at 48 hpf in wildtype (*c*) and sih^{b109} mutant (*d*) hearts. MF20 (TRITC) stains the entire heart tube and S46 (FITC) stains only the atrium. In double-exposure, the ventricle (v) fluoresces red and the atrium (a) fluoresces yellow. The stretched appearance of the mutant heart tube (*d*) is probably due to pericardial edema. Notably, even in the absence of contraction, the heart forms and loops normally.

[1]*Department of Biochemistry and Biophysics, Programs in Developmental Biology, Genetics and Human Genetics, University of California at San Francisco, 513 Parnassus Avenue, Box 0448, San Francisco, California 94143-0448, USA.* [2]*Department of Pediatrics, University of California at San Francisco, California, USA.* [3]*Laboratory of Molecular Genetics, National Institute of Child Health & Human Development, National Institutes of Health, Bethesda, Maryland, USA.* [4]*Institute of Neuroscience, University of Oregon, Eugene, Oregon, USA.* [5]*Cardiovascular Research Center, Massachusetts General Hospital, Boston, Massachusetts, USA. Correspondence should be addressed to D.Y.R.S. (e-mail: didier_stainier@biochem.ucsf.edu).*

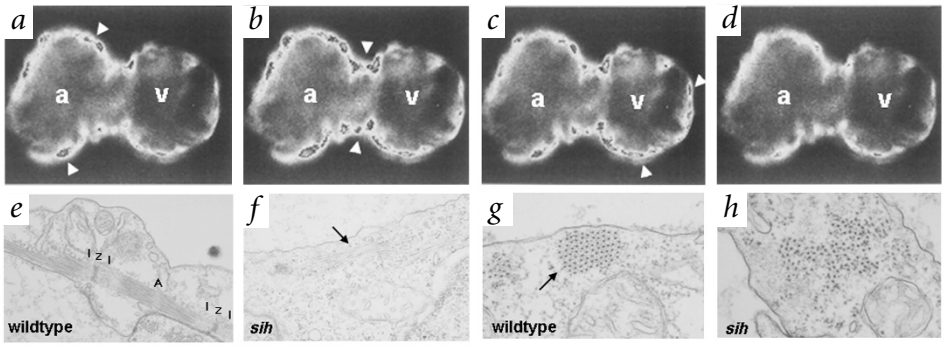

Fig. 2 *sih* mutant cardiomyocytes show normal cellular excitation, but have defective sarcomere assembly. ***a–d,*** In the *sih* mutant heart, Ca^{2+} entry into cardiomyocytes proceeded as a wave (arrowheads, *a–c*) starting in the atrium (a) and moving through the atrio-ventricular junction into the ventricle (v), before reaching a resting state (*d*). ***e,f,*** Longitudinal sections of wildtype (*e*) and sih^{b109} mutant (*f*) cardiomyocytes at 48 hpf as observed by electron microscopy. A-band, I-bands and Z-lines are visible in a wildtype sarcomere (*e*). The arrow in *f* points to disorganized thick filaments seen in sih^{b109} mutant cardiomyocytes. ***g,h,*** Cross-sections showing tightly bundled, hexagonal arrays of thick and thin filaments in a wildtype cardiomyocyte (arrow, *g*), and loosely scattered thick filaments, without intervening thin filaments, in a sih^{b109} mutant cardiomyocyte (*h*).

actin and α-actinin, the earliest Z-disk protein, also seem to be expressed at wildtype levels (Fig. 3*d* and data not shown). By contrast, thin-filament proteins of the tropomyosin–troponin (Tpma–Tn) complex are altered in *sih* mutant hearts. Expression of Tpma seems slightly reduced (Fig. 3*f*), and cardiac troponin T (Tnnt2) and Tnni3 are undetectable (Fig. 3*h*,*j*). Heterozygous *sih* embryos show no obvious reduction in protein expression. The Tpma–Tn complex contains regularly spaced troponin subunits that are anchored to Tpma and regulate contraction in response to calcium[5]. The *sih* mutation might directly affect expression of Tpma, Tnnt2 and Tnni3, or reduce expression of one of these proteins and secondarily cause instability or degradation of the others. Some precedence for such secondary effects exists in *Drosophila melanogoster* indirect flight-muscle mutants, where a lack of troponin T results in secondary reduction of tropomyosin and actin[11]. Because the cellular and molecular phenotypes of *sih* mutants most closely resemble those of troponin T mutants in flies, we pursued *tnnt2* as a candidate for the *sih* mutation, and in parallel mapped the *sih* gene.

We cloned zebrafish *tnnt2* by immunoscreening an adult zebrafish heart expression library (see Web Fig. A online). In wildtype embryos, *tnnt2* mRNA is expressed by the 15-somite stage (16.5 hpf) in the bilateral myocardial precursors (Fig. 4*a*) and continues to be expressed in a heart-restricted pattern throughout development (Fig. 4*c*,*e*,*g*). We found that *tnnt2* mRNA expression is severely reduced at all stages in *sih* mutant embryos from both alleles (Fig. 4*b*,*d*,*f*,*h*). *tpma* mRNA is expressed at wildtype levels in somites (Fig. 4*i–l*), but at a reduced level in the heart, at 24 hpf (arrowhead, Fig. 4*j*). This difference in cardiac expression becomes more exaggerated over time, whereas expression of *tpma* in somites remains normal (Fig. 4*k*,*l*). Considering the role of Tnnt2 in contraction and its absence in mutant hearts, we hypothesized that the *sih* phenotype results primarily from reduction in *tnnt2* expression.

Given the described cellular and molecular phenotypes of *sih*, we tested whether the *sih* gene product functions within cardiomyocytes. Using cell transplantation to generate genetic mosaics, we found that when wildtype cells contribute to mutant hearts, they contract spontaneously and express Tnnt2 (see Web Fig. B, and Web Movie B and Web Note B online). Thus, the *sih* gene product acts in a cell-autonomous manner in regulating cardiomyocyte contractility and Tnnt2 expression. Next, we used morpholino antisense technology to 'knock-down' Tnnt2 translation[12]. Injection of a *tnnt2*-specific morpholino oligonucleotide into wildtype eggs resulted in the absence of Tnnt2 protein expression and non-contractile embryonic heart in 98% (230/234) of injected embryos. In addition, immunohistochemistry on morpholino-injected

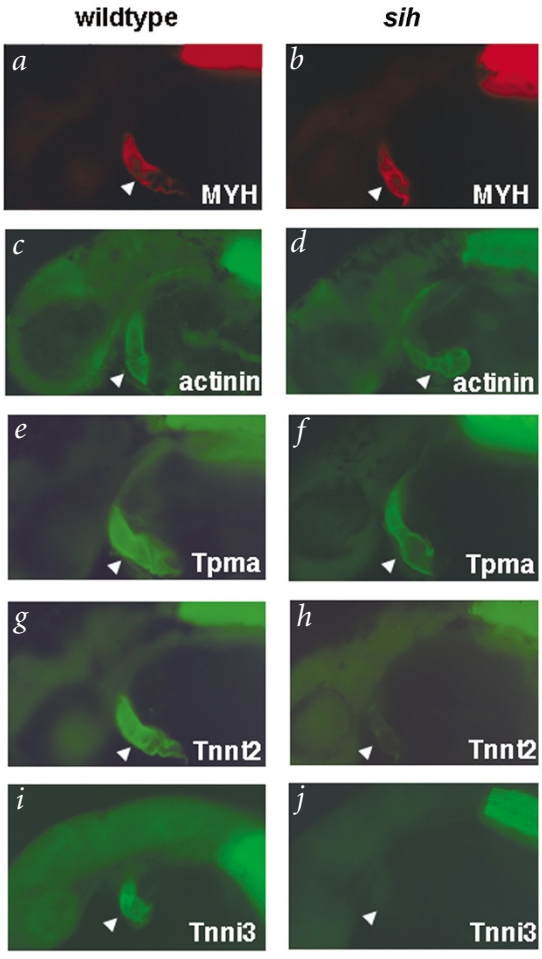

Fig. 3 Reduced protein expression of Tpma, Tnnt2 and Tnni3 in *sih* mutant hearts. All panels show results from the sih^{b109} allele; sih^{tc300b} mutants show exactly the same phenotype. ***a–j,*** Lateral views, anterior to the left, dorsal to the top, heart (arrowhead). Stains: myosin heavy chain, MF20-TRITC (*a*,*b*), α-actinin-FITC (*c*,*d*), Tpma, CH1-FITC (*e*,*f*), Tnnt2, JLT-12-FITC (*g*,*h*) and Tnni3, IE7-FITC (*i*,*j*). The same wildtype embryo is shown in *a* and *g*, and the same mutant embryo is shown in *b* and *h*. Staining is also evident in skeletal muscle and serves as an internal control. Embryos were fixed at 30–32 hpf, except those shown in *i* and *j*, which were fixed at 24 hpf.

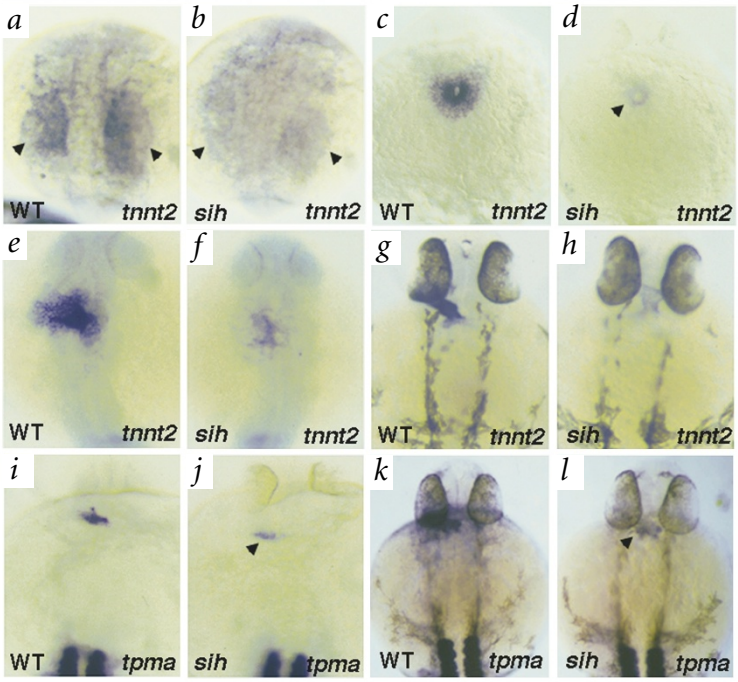

Fig. 4 Severely reduced *tnnt2* mRNA expression in *sih* mutant embryos throughout development. ***a–h***, All panels show the sih^{b109} allele, dorsal views, anterior to the top; sih^{tc300b} mutants have the same phenotype. *a*,*c*,*e*,*g*, Wildtype *tnnt2* expression. *b*,*d*,*f*,*h*, Reduced expression in *sih* mutant embryos. At the 15-somite stage (16.5 hpf), *tnnt2* expression was not detected above background levels in the mutant lateral plate mesoderm (arrowheads, *b* versus *a*). By cone formation (21 somites), some faintly expressing cells were seen around the central lumen (arrowhead, *d* versus *c*). During heart tube elongation (24 hpf, *f*) and looping (30 hpf, *h*), an increasing number of expressing cells were detected in mutant embryos, but the level of expression in these cells remained severely reduced compared with the wild type (*e*,*g*). ***i–l***, Progressive reduction in *tpma* mRNA expression in *sih* mutant hearts. At 24 hpf, *tpma* was detected at a reduced level in *sih* mutant hearts (arrowhead, *j*) compared with wildtype hearts (*i*). This reduction of *tpma* expression in mutant hearts became even more pronounced over time (30 hpf, *l* versus *k*). Note that *tpma* is expressed heavily in the somites at both stages. Transcript levels of *cmlc2*, a thick filament component, seem normal in *sih* mutant hearts (data not shown).

embryos revealed a slight reduction of Tpma and absence of Tnni3 in a pattern identical to that seen in *sih* mutant embryos (data not shown). Thus, a lack of Tnnt2 phenocopies the *sih* mutation and results in misexpression of other proteins of the Tpma–Tn complex. These findings indicate that Tnnt2 is essential in sarcomere assembly.

We mapped *sih* and *tnnt2* to the same region of linkage group 23 (Fig. 5*a*). We assembled a small contiguous stretch of PACs and used fine-scale recombinant mapping to locate the *sih* locus on PAC 65I4, which also contained *tnnt2* (ref. 13). Genotyping embryos for a polymorphic marker within the 5′ upstream sequence of *tnnt2* revealed no recombination in 2,095 meiotic events between this marker and the *sih* locus. Injection of PAC 65I4 DNA into embryos from *sih* heterozygote intercrosses yielded six mosaically transgenic mutant embryos, where a subset of cells could be seen beating in otherwise non-contractile hearts (see Web Movie C and Web Note C online). The rescued cells also expressed Tnnt2 (Fig. 5*b*,*c*). Together, the tight genetic linkage, morpholino phenocopy and rescue experiments provide genetic evidence that *sih* encodes Tnnt2.

Genomic sequencing of the two *sih* mutated alleles revealed noncoding mutations in *tnnt2*. The sih^{tc300b} mutation results in an A→G change at the invariant –2 position of the splice-acceptor sequence in intron 2 and leads to pleiotropic defects in mRNA splicing. The most common transcript amplified by RT–PCR uses a cryptic splice-site that results in partial exclusion of exon 3 and a frameshift that leads to a premature stop codon in exon 7 (Fig. 5*d*). This mutation results in severely reduced *tnnt2* expression, probably through nonsense-mediated mRNA decay[14,15]. The sih^{b109} mutation causes a deletion of 13 bp in the 5′ non-transcribed region of *tnnt2* (Fig. 5*e*). To evaluate the effect of this deletion on *tnnt2* expression, we carried out *in vivo* promoter analyses. An upstream gene fragment (–308) was cloned into a reporter vector encoding green fluorescent protein (GFP) and injected into wildtype embryos. On average, 17% of the injected embryos showed a mosaic pattern of intense, heart-specific GFP fluorescence (Fig. 6*b*,*c*). By contrast, no fluorescing cells were seen when a sih^{b109} mutant promoter construct (–308 Δ13) was

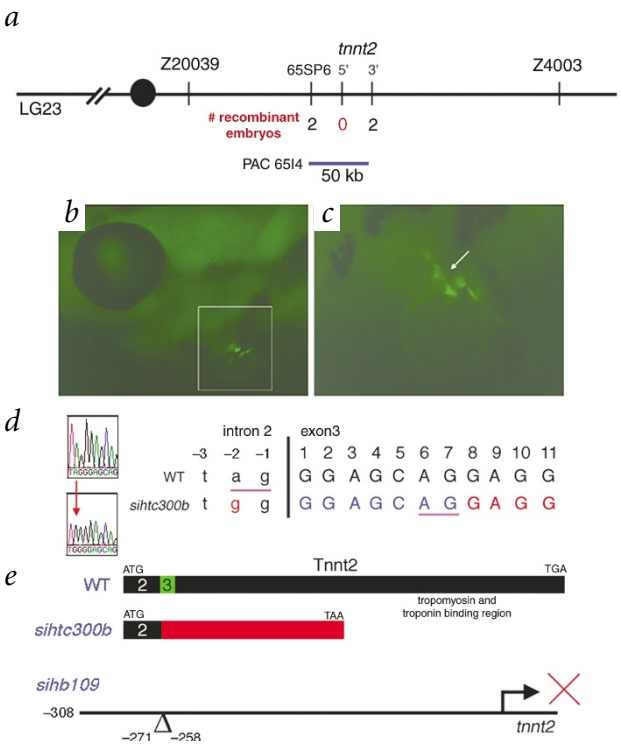

Fig. 5 *sih* encodes Tnnt2. ***a***, Linkage. Genotyping of sih^{b109} mutant embryos shows recombinants for RFLPs on the telomeric (*tnnt2* 3′ UTR; 2 in 2,095 meiotic events) and centromeric (PAC-end (65SP6); 2 in 1,872 meiotic events) sides of the *sih* locus. No recombinants were found for an SSCP in the 5′ upstream sequence of *tnnt2*. The two recombinants on the telomeric side represent intragenic recombination events. PAC 65I4 (50 kb) contains *tnnt2* and spans the *sih* locus. ***b***,***c***, PAC rescue of a sih^{b109} mutant embryo; panels show lateral view, anterior to the left. Rescued cardiac cells (area of detail, *b*) express Tnnt2 (arrow, *c*). ***d***,***e***, Genetic defects in the two *sih* mutated alleles. ***d***, An A→G change at the –2 position of the splice-acceptor sequence in intron 2 was identified in the sih^{tc300b} allele by genomic sequencing. Consensus splice site in wildtype sequence (ag) is shown. The utilization of a downstream cryptic splice site in sih^{tc300b} mutants (AG) results in a partial exclusion of 7 bp of exon 3 (blue bases) and a frameshift (red) that leads to a premature stop codon in exon 7 (TAA). Only the first 11 aa of Tnnt2 (exon 2) are encoded by this mutant message. ***e***, A deletion of 13 bp from nt –258 to nt –271 of *tnnt2* is found in sih^{b109} mutants (see Web Fig. A online for the complete upstream sequence).

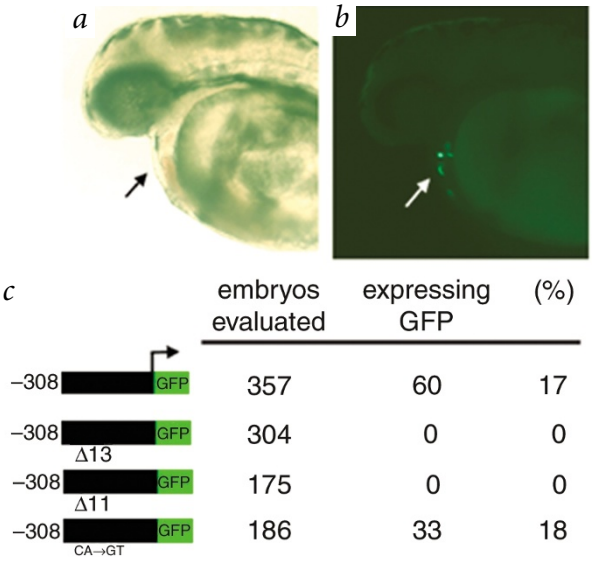

Fig. 6 The *sih*^{b109} promoter deletion abolishes reporter expression *in vivo*. ***a***,***b***, Lateral view of head and heart (arrow, *a*) in a transient transgenic zebrafish embryo. Five GFP-expressing cells are seen (arrow, *b*). ***c***, Data table shows the number of injected embryos evaluated for GFP expression using the wildtype (–308), *sih*^{b109} (–308 Δ13), 11-bp deletion (–308 Δ11) and E-box mutation (CA→GT) constructs. No GFP expression is observed when mutant deletion constructs are injected. GFP expression occurs at wildtype levels when the E-box mutation construct is injected. However, GFP expression was not heart-specific in 5 of 33 expressing embryos using this construct. Results are a summation of independent injection experiments.

injected (Fig. 6*c*). Moreover, injection of an 11-bp deletion construct (–308 Δ11), which corrects for phase in the DNA helix, did not rescue reporter expression (Fig. 6*c*). To determine whether this mutation could directly disrupt a critical *cis*-regulatory element, we examined the sequence of the 13-bp deletion and identified a consensus E-box transcription factor binding site (CANNTG)[16]. When the first two bases of the E-box were changed from CA to GT and the mutated reporter construct was injected into embryos, 33 (18%) of them expressed GFP in the heart (Fig. 6*c*). This number is essentially identical to the number obtained when using the wildtype promoter construct, with the notable exception that ectopic GFP expression was seen in 5 of the 33 embryos (that is, 1 or 2 fluorescing cells in the body, bloodstream, and/or head). Thus, although the identified E-box may not be necessary for *tnnt2* expression, bases within this region may be relevant to heart-specific expression of *tnnt2*. From these data, we propose that the deletion of 13 bp causes a severe reduction in *tnnt2* transcription in *sih*^{b109} mutant embryos; its effect on the binding of critical transcriptional complexes warrants future investigation.

The mutations reported here provide the first animal model of Tnnt2 deficiency. Without Tnnt2, cardiac sarcomeres fail to assemble and heart muscle is rendered nonfunctional. Reduction of Tnnt2 is accompanied by reductions in Tpma and Tnni3. A reduction in *tpma* mRNA in *sih* mutant hearts indicates the existence of a feedback mechanism to tightly coordinate the expression of these interrelated proteins. In humans, hypertrophic cardiomyopathy resulting from dominant mutations in *TNNT2* can cause sudden death without evidence of clinical hypertrophy[17]. The precise molecular mechanisms leading to sudden death are unknown. A recent histopathological study of nine hearts from individuals with *TNNT2* mutations reported lower heart weights, greater myocyte disarray and less fibrosis than hearts from individuals with hypertrophic cardiomyopathy of unknown genotype[6]. There may thus be a link between *TNNT2* mutations, myocyte disarray and ischemia as risk factors for sudden cardiac death.

In transgenic mice, a human splice-site mutation that results in a carboxy-terminal Tnnt2 truncation has been modeled[18]. Only mice expressing less than 5% of total Tnnt2 as the truncated form survive beyond 24 hours; these mice have fewer and smaller cardiomyocytes and decreased heart mass. The truncated Tnnt2 molecule shows altered stability within the sarcomere and causes misregistration of Z-bands and myofibrillar disarray and degeneration[7]. Mechanical dysfunction due to incorporation of the abnormal protein was proposed as the mechanism leading to structural breakdown of sarcomeres and possibly increased apoptosis. Alternatively, based on the loss-of-function data presented here, we propose that if a mutation in *TNNT2* results in the reduced expression of other proteins of the Tpma–Tn complex, then defective sarcomeres would be directly eliminated and lead to myocyte disarray. Identifying the multilevel controls that regulate contractile protein expression is key to understanding cardiomyocyte function and dysfunction.

Methods

Zebrafish. We maintained and staged zebrafish as described[19]. The *sih*^{b109} mutation was identified in a γ-ray mutagenesis screen in the laboratory of Charles Kimmel (Eugene, Oregon).

Calcium activation. We dissected hearts from wildtype and *sih*^{b109} embryos at 32 hpf and loaded them with Ca^{2+} green (Molecular Probes) according to the manufacturer's instructions. We then viewed and recorded the hearts using a Zeiss Axiophot microscope.

Electron microscopy. We fixed wildtype and homozygous mutant *sih*^{b109} embryos at 48 hpf in 2% glutaraldehyde in 0.1M sodium cacodylate buffer (pH 7.2). Post-fixation was carried out in 0.5% OsO_4 plus 0.8% $K_3Fe(CN)_6$. We then placed embryos in 2% uranyl acetate for 1 h in the dark and dehydrated them in a graded acetone solution. We used Epon-Araldite resin for embedding and cured the resin for 48 h at 60 °C. We cut thin sections (70 nm), post-stained them with uranyl acetate and lead citrate and observed them under a JEOL 100CX electron microscope.

Immunohistochemistry. We carried out whole-mount immunohistochemistry as described[20]. We used monoclonal antibodies against myosin heavy chain, MF20 (ref. 21); atrial-specific myosin heavy chain, S46 (gift from F. Stockdale, Stanford Univ.); α-actinin (Sigma); tropomyosin, CH1 (ref. 22); cardiac troponin T, JLT12 (Sigma); cardiac troponin I, IE7 (gift from J. Potter, Univ. of Miami); and α-sarcomeric actin (Sigma). Anti-IgG2b TRITC recognized MF20. FITC conjugated anti-mouse antibodies recognized S46, α-actinin, CH1 and JLT12 (IgG1-FITC), IE7 (IgG-FITC) and α-sarcomeric actin (IgM-FITC).

Isolation of *tnnt2* cDNA. We used a heart-specific monoclonal antibody against Tnnt2, mAb13-11 (ref. 23; gift from P. Anderson, Duke Univ.) to screen 5×10^5 recombinants from a zebrafish heart cDNA library in Stratagene Uni-ZAP XR (gift from R. Breitbart). We applied nitrocellulose filters impregnated with isopropyl-b-D-thiogalactopyranoside to plaques for 4 h at 37 °C. We blocked filters (3% nonfat dry milk in Tris buffered saline with 0.1% tween) and then incubated them in mAb13-11 (1:2,000). After washes we incubated filters with a goat anti-mouse HRP conjugated secondary antibody (1:5,000). We carried out electro-chemi-luminescence detection with ECL reagents (Amersham). Positive pBluescript phagemids were *in vivo* excised and sequenced. Sequencing of three clones revealed identical, full-length cDNA sequences that have significant homology to other vertebrate *tnnt2* genes (see Web Fig. A online).

***In situ* hybridization.** We carried out whole-mount *in situ* hybridization as described[20]. We used antisense RNA probes to zebrafish *tnnt2*, *cardiac myosin light chain 2* (*cmlc2*)[24] and *tpma*[25].

Morpholino antisense 'knock-down'. We designed a morpholino oligonucleotide (Gene Tools) to bind the Tnnt2 translation start codon and flanking 5′ sequence (5′-CATGTTTGCTCTGATCTGACACGCA-3′). We injected 4 ng of the morpholino oligo into embryos at the 1–4 cell stage and examined the cardiac phenotype of the injected embryos at 30 hpf.

Genetic mapping. We genotyped a combination of diploid mutant embryos and haploid mutant and wildtype embryos from *sih*^{b109} AB/WIK hybrid strains on the telomeric side of the *sih* locus using a restriction fragment length polymorphism (RFLP) in the 3′ UTR of *tnnt2*. We isolated PAC 65I4 by PCR from PAC library pools using *tnnt2*-specific primers and sized it on a pulse-field gel[13]. We directly sequenced the PAC ends. We used an RFLP in one end of the PAC (65SP6) to genotype on the centromeric side of the *sih* locus. We then obtained 5′ upstream sequence of *tnnt2* by direct PAC sequencing and used a single-strand conformation polymorphism (SSCP) within this sequence for final genotyping of all recombinant embryos.

Mutation detection. We used pools of 100 homozygous mutant embryos from both alleles (*sih*^{b109} and *sih*^{tc300b}) to extract mRNA (Trizol, Gibco BRL) and synthesize cDNA (SuperScript II Reverse Transcription, Gibco BRL). We amplified and cloned two overlapping fragments of *tnnt2* coding region from the cDNA pools. Sequencing of clones from the *sih*^{tc300b} allele revealed one abnormally spliced transcript, which contained sequence for intron 2, and three independent clones of a second splice form, which partially excluded exon 3. The splice form that contained intron 2 had a G at the –2 position of the splice-acceptor sequence (consensus=A). We confirmed an A→G change at this position by sequencing two independent clones amplified from mutant genomic DNA (DNA). Coding sequence analysis of the *sih*^{b109} allele revealed no mutations. We therefore amplified and cloned a 327-bp fragment of *tnnt2* 5′ upstream sequence (containing the SSCP described above) from genomic DNA prepared from individual wildtype and *sih*^{b109} haploid embryos. We identified a deletion of 13 bp from nt –258 to nt –271 upstream of the transcription start site, which we confirmed in three independent clones from *sih*^{b109} embryos.

Phenotypic rescue. We isolated PAC DNA using a Maxi-Kit (Qiagen) and injected it at concentrations ranging from 50 μg ml^{-1} to 190 μg ml^{-1} into embryos from *sih*^{b109} and *sih*^{tc300b} heterozygote intercrosses. At 30 hpf, we sorted mutant embryos and observed them for evidence of beating cells in the heart. We then prepared injected embryos for whole-mount immunohistochemistry using antibody mAB13-11 (ref. 23). We genotyped rescued embryos from the *sih*^{b109} allele using an allele-specific RFLP that lies outside of the PAC.

Promoter analysis. We amplified a 327-bp fragment from nt –308 to nt +19 of *tnnt2* (see Web Fig. A online) from homozygous wildtype WIK and *sih*^{b109} genomic DNA and cloned it into the pEGFP-1 promoterless reporter vector (Clontech). We used the QuikChange Site-Directed Mutagenesis Kit (Stratagene) to generate two additional constructs using the mutant (–308 Δ13) and wildtype (–308) constructs as templates, respectively. To create an 11-bp deletion (–308 Δ11), we re-inserted two bases (GG) into the (–308 Δ13) construct. To alter the E-box consensus site (CANNTG) contained within the 13-bp sequence, we changed two bases within the wildtype promoter (CA to GT). We confirmed all constructs by sequencing. We diluted plasmid DNA to a working concentration of 100 μg ml^{-1} for microinjection. We scored injected embryos for GFP expression at 30–48 hpf.

GenBank accession numbers: Zebrafish *tnnt2*, AF282384; PAC 65I4, AL662878.

Note: Supplementary information is available on the Nature Genetics website.

Acknowledgments

We thank A. Navarro and S. Waldron for their dedicated care of our fish, K. MacDonald for his expertise in generating electron micrographs, and M. Brook and F. Aburto for their assistance with the Quicktime movies. We thank C. Kimmel, F. Stockdale, J. Potter, P. Anderson and R. Breitbart for sharing valuable reagents; W. Tidyman, C. Ordahl and B. Black for helpful discussions about cardiac gene regulation and P. Wolters, M. Zeiger, R. Reijo-Pera and members of the Stainier lab for their comments on this manuscript. A.S. was supported as a March of Dimes fellow of the Pediatric Scientist Development Program and by the American Heart Association Western States Affiliate. This work was supported in part by grants from the National Institutes of Health (to A.S., M.C.F. and D.Y.R.S., and to Charles Kimmel supporting the mutagenesis screen), as well as grants from the Packard Foundation and the American Heart Association (to D.Y.R.S.).

Competing interests statement

The authors declare that they have no competing financial interests.

Received 29 June 2001; accepted 15 March 2002

1. Thierfelder, L. *et al*. α-tropomyosin and cardiac troponin T mutations cause familial hypertrophic cardiomyopathy: a disease of the sarcomere. *Cell* **77**, 701–712 (1994).
2. Maron, B.J. *et al*. Sudden death in young competitive athletes. Clinical, demographic, and pathological profiles. *JAMA* **276**, 199–204 (1996).
3. Seidman, J.G. & Seidman, C. The genetic basis for cardiomyopathy: from mutation identification to mechanistic paradigms. *Cell* **104**, 557–567 (2001).
4. Kamisago, M. *et al*. Mutations in sarcomere protein genes as a cause of dilated cardiomyopathy. *N. Engl. J. Med.* **343**, 1688–1696 (2000).
5. Tobacman, L.S. Thin filament-mediated regulation of cardiac contraction. *Annu. Rev. Physiol.* **58**, 447–481 (1996).
6. Varnava, A.M. *et al*. Hypertrophic cardiomyopathy: histopathological features of sudden death in cardiac troponin T disease. *Circulation* **104**, 1380–1384 (2001).
7. Tardiff, J.C. *et al*. Cardiac troponin T mutations result in allele-specific phenotypes in a mouse model for hypertrophic cardiomyopathy. *J. Clin. Invest.* **104**, 469–481 (1999).
8. Chen, J.N. *et al*. Mutations affecting the cardiovascular system and other internal organs in zebrafish. *Development* **123**, 293–302 (1996).
9. Stainier, D.Y. *et al*. Mutations affecting the formation and function of the cardiovascular system in the zebrafish embryo. *Development* **123**, 285–292 (1996).
10. Burggren, W.W. & Pinder, A.W. Ontogeny of cardiovascular and respiratory physiology in lower vertebrates. *Annu. Rev. Physiol.* **53**, 107–135 (1991).
11. Fyrberg, E., Fyrberg, C.C., Beall, C. & Saville, D.L. *Drosophila melanogaster* troponin-T mutations engender three distinct syndromes of myofibrillar abnormalities. *J. Mol. Biol.* **216**, 657–675 (1990).
12. Nasevicius, A. & Ekker, S.C. Effective targeted gene 'knockdown' in zebrafish. *Nature Genet.* **26**, 216–220 (2000).
13. Amemiya, C.T., Zhong, T.P., Silverman, G.A., Fishman, M.C. & Zon, L.I. Zebrafish YAC, BAC, and PAC genomic libraries. *Methods Cell Biol.* **60**, 235–258 (1999).
14. O'Neill, J.P., Rogan, P.K., Cariello, N. & Nicklas, J.A. Mutations that alter RNA splicing of the human HPRT gene: a review of the spectrum. *Mutat. Res.* **411**, 179–214 (1998).
15. Maquat, L.E. & Carmichael, G.G. Quality control of mRNA function. *Cell* **104**, 173–176 (2001).
16. Edmondson, D.G. & Olson, E.N. Helix-loop-helix proteins as regulators of muscle-specific transcription. *J. Biol. Chem.* **268**, 755–758 (1993).
17. Moolman, J.C. *et al*. Sudden death due to troponin T mutations. *J. Am. Coll. Cardiol.* **29**, 549–555 (1997).
18. Tardiff, J.C. *et al*. A truncated cardiac troponin T molecule in transgenic mice suggests multiple cellular mechanisms for familial hypertrophic cardiomyopathy. *J. Clin. Invest.* **101**, 2800–2811 (1998).
19. Westerfield, M. *The Zebrafish Book* (Univ. of Oregon Press, Eugene, 1995).
20. Alexander, J., Stainier, D.Y. & Yelon, D. Screening mosaic F1 females for mutations affecting zebrafish heart induction and patterning. *Dev. Genet.* **22**, 288–299 (1998).
21. Bader, D., Masaki, T. & Fischman, D.A. Immunochemical analysis of myosin heavy chain during avian myogenesis *in vivo* and *in vitro*. *J. Cell. Biol.* **95**, 763–770 (1982).
22. Lin, J.J., Chou, C.S. & Lin, J.L. Monoclonal antibodies against chicken tropomyosin isoforms: production, characterization, and application. *Hybridoma* **4**, 223–242 (1985).
23. Malouf, N.N., McMahon, D., Oakeley, A.E. & Anderson, P.A. A cardiac troponin T epitope conserved across phyla. *J. Biol. Chem.* **267**, 9269–9274 (1992).
24. Yelon, D., Horne, S.A. & Stainier, D.Y. Restricted expression of cardiac myosin genes reveals regulated aspects of heart tube assembly in zebrafish. *Dev. Biol.* **214**, 23–37 (1999).
25. Ohara, O., Dorit, R.L. & Gilbert, W. One-sided polymerase chain reaction: the amplification of cDNA. *Proc. Natl Acad. Sci. USA* **86**, 5673–5677 (1989).